

## Experimental demonstration of a high-power slow-wave electron cyclotron maser based on a combined resonance of Cherenkov and anomalous Doppler interactions

K. Ogura,<sup>1</sup> M. R. Amin,<sup>1</sup> K. Minami,<sup>1</sup> X. D. Zheng,<sup>1</sup> Y. Suzuki,<sup>1</sup> W. S. Kim,<sup>1</sup>  
T. Watanabe,<sup>2</sup> Y. Carmel,<sup>3</sup> and V. L. Granatstein<sup>3</sup>

<sup>1</sup>Graduate School of Science and Technology, Niigata University, Niigata 950-21, Japan

<sup>2</sup>National Institute for Fusion Science, Nagoya 464-01, Japan

<sup>3</sup>Institute for Plasma Research, University of Maryland, College Park, Maryland 20742

(Received 10 August 1995)

A slow-wave electron cyclotron maser consisting of an oversized corrugated waveguide and an axially injected electron beam has been demonstrated experimentally. At resonance, the output rf power is strongly enhanced. Maximum output power of 200 kW with an electronic efficiency of 4% at 19.5 GHz is obtained for an electron beam with voltage of 35 kV and current of 150 A. The oscillation is observed to be a periodic  $TM_{01}$  mode. The enhancement of microwave radiation is estimated to be caused by the combined resonance of Cherenkov interactions and an anomalous Doppler shifted electron cyclotron interaction.

PACS number(s): 41.60.Bq, 84.40.Ik, 52.75.Va, 84.40.Fe

### I. INTRODUCTION

Cyclotron and Cherenkov interactions between electrons and electromagnetic waves have been successfully utilized in high-power microwave devices [1]. In electron cyclotron masers (ECM's) such as gyrotrons and cyclotron autoresonance masers [2,3], normal modes of a cavity have their phase velocity  $v_{ph}$  higher than the speed of light in vacuum  $c$ . These fast wave modes interact with a fast cyclotron wave on the electron beam at the normal Doppler shifted frequency,  $\omega = k_z v_z + S\Omega$ . Here,  $\Omega$  is the angular electron cyclotron frequency,  $S$  is a positive integer,  $k_z$  is the axial wave number, and  $v_z$  is the axial electron velocity. In these fast-wave devices, the perpendicular velocity of the injected beam is a crucial parameter to be adjusted carefully to obtain a high beam-to-rf conversion efficiency. However, it is difficult to control both the axial and transverse velocities of the beam simultaneously. In the Cherenkov devices such as the backward wave oscillator and its special variants [4–6], slow space charge waves interact with the slow electromagnetic modes of the cavity. These devices can be driven by an axially injected electron beam without initial perpendicular velocity and are particularly suited to operation with an intense electron beam.

It has been suggested that an ECM operating in the Cherenkov regime ( $v_{ph} < c$ ) may be an attractive alternative high-power microwave source [7–9]. This slow-wave ECM utilizes the coupling between the slow cyclotron waves on the beam and the slow electromagnetic waves of the cavity at the anomalous Doppler cyclotron resonance,  $\omega = k_z v_z + S\Omega$  with  $S = -1$  or any other negative integer. Such a slow-wave ECM can be driven by an electron beam with predominant axial velocity as in conventional Cherenkov devices. Experimental demonstrations of the high-power slow-wave ECM's were reported in Refs. [10], [11], and [12], in which dielectric loaded or co-

axial type of slow-wave structure (SWS) was used.

In the slow-wave ECM operating in the Cherenkov regime, the anomalous Doppler and Cherenkov interactions may compete with each other and must be controlled carefully [13]. The results of the computer simulation in Ref. [13] indicate that the Cherenkov instability can be suppressed by the rapid growth rate of the anomalous Doppler cyclotron instability in the high-voltage or the high-current regime. In the slow-wave ECM experiment of Ref. [12], the length of the dielectric loaded SWS was limited in order to keep the Cherenkov emission at low level.

In this paper, we demonstrate experimentally that the slow cyclotron and Cherenkov instabilities can be combined favorably to generate high-power microwave radiations in a moderate beam voltage and current regime, less than 50 kV and on the order of 100 A, respectively. Our high-power slow-wave ECM consists of a sinusoidally corrugated metallic SWS, which is oversized with the mean diameter four times larger than the free space wavelength  $\lambda$  of the microwave output for  $TM_{01}$  mode. The parameters of the SWS are as follows; average radius  $R_0 = 30$  mm, corrugation amplitude  $h = 1.7$  mm, pitch length  $z_0 = 3.4$  mm, and the total length  $L = 70z_0 = 238$  mm.

A detailed analysis of the starting condition for the Cherenkov oscillation using our SWS is presented in Ref. [14] and the results are summarized here. In order to sustain the Cherenkov oscillation with the finite length SWS, there exist two threshold conditions on the beam current and energy. The former is well known as an oscillation starting current. The latter is the starting energy due to the finite interaction space. The oscillation condition in the SWS with an axial length  $L$  demands a finite width of the interaction region, on the order of  $2\pi/L$ , in wave-number space. This condition cannot be satisfied by increasing the beam current only. By increasing beam energy, the Cherenkov interaction point approaches the

upper edge of the transmission band and the interaction width in wave-number space becomes broad enough to satisfy the oscillation condition. For our SWS, the theoretically predicted starting energy is about 75 keV [14]. Preliminary experiments on the Cherenkov oscillation, which are now under way, indicate that the threshold beam voltage is above about 50 kV.

## II. EXPERIMENT

A schematic diagram of the experimental setup is shown in Fig. 1. The electron-beam diode, the SWS, and the beam collector are installed in a stainless steel vacuum vessel. The axial magnetic field is uniform from the cathode to the end of the SWS. The axisymmetric emitting edge of the cathode is wrapped with velvet. The diode voltage is measured by a capacitive voltage divider. For measurements of beam current, a Rogowski coil is placed at an entrance of the SWS. The receiving antenna is a rectangular horn antenna. The coupling coefficients between the output window and the receiving antenna are determined by a vector network analyzer for a circular  $TM_{01}$  mode. The absolute values of the output microwave power are estimated by using these coupling coefficients.

The output power from the slow-wave ECM strongly depends on the magnetic field as is shown in Fig. 2. The measured diode voltage and beam current are  $35 \pm 5$  keV and  $150 \pm 40$  A, respectively. Time histories of diode voltage and beam current are shown in the inset of Fig. 2. Off resonance, less than about 0.7 T, no meaningful microwave power is observed. The microwave power increases resonantly with magnetic field and maximum output power of about 200 kW is obtained. This corresponds to an electronic efficiency of about 4%. When the SWS is replaced by a straight cylindrical waveguide, the detected power remains in the noise level as shown by the triangles in Fig. 2.

Microwave output signals with and without a delay line are compared in Fig. 3(a). The shape of the delayed pulse is similar to that of the prompt pulse, indicating that the slow-wave ECM operates at a single mode of the SWS. The observed frequency is  $19.5 \pm 0.5$  GHz for the magnetic field ranging from 0.75 to 0.98 T in Fig. 2. By increasing the beam voltage from  $35 \pm 5$  kV to  $50 \pm 6$  kV, the frequency changes to  $21 \pm 0.5$  GHz for the same re-

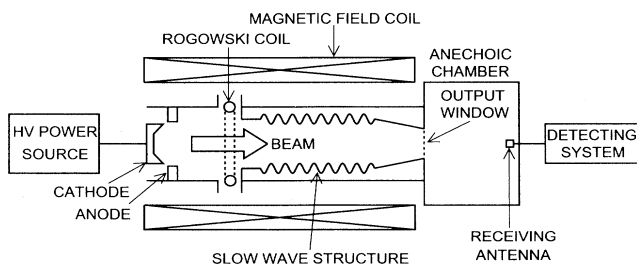


FIG. 1. Schematic diagram of the experimental setup.

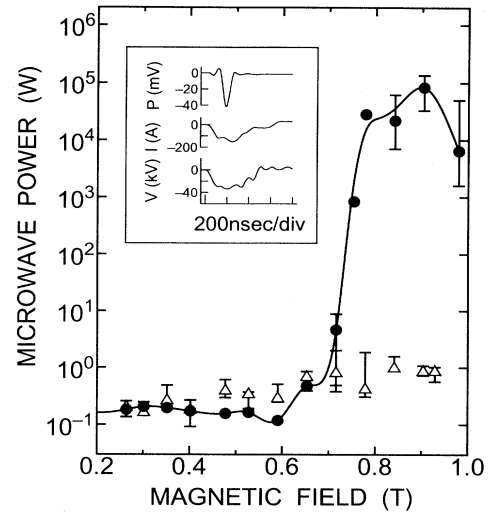


FIG. 2. Microwave output power vs applied axial magnetic field. Closed circles connected by solid line show absolute output powers of the slow-wave ECM. Open triangles are output powers when the periodic SWS is replaced by the straight cylinder waveguide with the same radius as the mean radius of the SWS. Inset shows the timing and wave forms of detected voltage of microwave power  $P$ , beam current  $I$ , and beam voltage  $V$ .

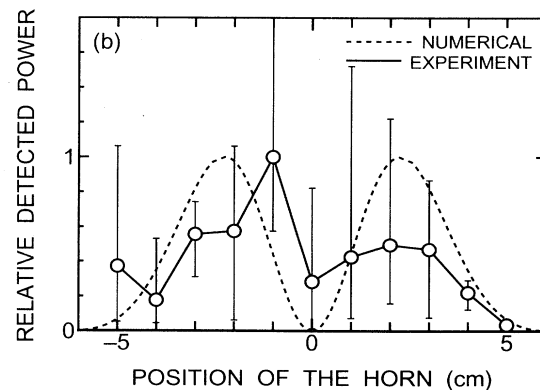
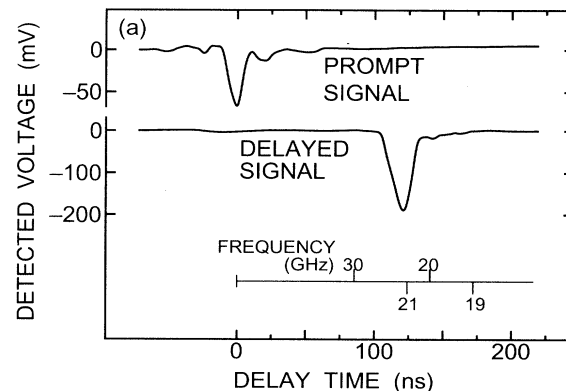


FIG. 3. (a) A typical shot of microwave signals. The delayed signal is obtained by using a 20-m-long waveguide delay line. (b) Radiation pattern of the output microwave obtained by scanning the receiving antenna vertically from the axis of the slow wave ECM.

gion of the magnetic field. A key parameter that determines the oscillation frequency is the beam voltage, not the magnetic field. The radiation pattern shown in Fig. 3(b) is measured by moving the receiving antenna vertically with the vertical electric polarization. By rotating the receiving antenna around its axis by 90°, the detected power level was decreased by a factor of five or more. The measured radiation pattern and its polarization indicate that the dominant radiation mode is the  $TM_{01}$  mode.

### III. DISCUSSION

In what follows, we discuss possible mechanisms for the resonant microwave radiation observed above. The dispersion characteristic of the periodic  $TM_{01}$  mode in the oversized SWS is shown in Fig. 4. For a magnetized electron beam, there exist three distinct beam waves, which can contribute microwave generations. They are the slow and the fast cyclotron waves and the beam space charge wave. The condition for the Cherenkov synchronism is

$$\omega(k_C) = k_C v_z, \quad (1)$$

where  $k_C$  is axial wave number at the point  $C$  in Fig. 4. For simplicity, the space charge effect is neglected. The cyclotron interaction conditions between the beam and the periodic  $TM_{01}$  modes are

$$\omega(k) = k v_z + S\Omega, \quad k = k_A \text{ and } k_D, \quad (2)$$

where  $k_A$  and  $k_D$  are the axial wave number at points  $A$  and  $D$  in Fig. 4, respectively. Points  $A$  and  $D$  respectively correspond to the anomalous Doppler cyclotron resonance with  $S = -1$  and the normal Doppler cyclotron resonance with  $S = 1$ . The conditions (1) and (2) are satisfied simultaneously at three distinct resonant magnetic fields,  $B$ , for the fundamental cyclotron resonances ( $S = \pm 1$ ) defined by

$$B = 2(k_0 - k_C) \frac{m}{e} \gamma v_z, \quad (3)$$

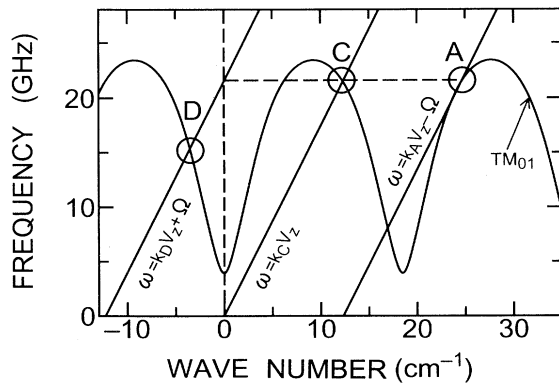


FIG. 4. The dispersion characteristics of the slow-wave ECM at the axial magnetic field of 0.76 T for the beam energy of 35 keV.

$$B = (2k_0 - k_C) \frac{m}{e} \gamma v_z \quad (4)$$

and

$$B = k_0 \frac{m}{e} \gamma v_z, \quad (5)$$

where  $k_0$  is the corrugation wave number,  $m$  is the electron mass,  $e$  is the elementary electric charge and  $\gamma$  is the relativistic factor.

Figure 4 corresponds to the combined resonance defined by Eq. (3). The Cherenkov instability at the point  $C$  is an absolute instability and oscillation can start from a noise. This signal can be amplified at the point  $A$  by the anomalous Doppler cyclotron interaction ( $S = -1$ ), which also offers a favorable positive feedback mechanism because group velocities of the  $TM_{01}$  mode at two points are opposite to each other. For a 35-keV beam, the estimated resonant magnetic field is 0.75 T, which is close to the experimental value in Fig. 2. It is expected that the oscillation frequency is determined by the Cherenkov interaction and does not depend on the magnetic field. An experimentally observed frequency change from  $19.5 \pm 0.5$  GHz with  $35 \pm 5$ -kV beam voltage to  $21 \pm 0.5$  GHz with  $50 \pm 6$ -kV beam voltage is in accordance with the predicted movement of the Cherenkov intersection point.

The admissible mismatch of two interactions at the combined resonance may be given by the condition that  $|\omega(k_C) - \omega(k_A)|T \leq 2\pi$ , where  $T$  is the transit time of the electron in the interaction region (see, for example, Chap. 2 of Ref. 1 and Ref. 3). Therefore, in order to maintain the combined resonance condition, the changes in beam voltage,  $\Delta V/V$ , may be on the order of [15]

$$\frac{\Delta V}{V} \leq \frac{(\gamma + 1)^2}{\gamma} \frac{eV}{mc^2} \frac{\lambda}{L(\beta_{g1} + \beta_{g2})}, \quad (6)$$

where  $\beta_{g1}, \beta_{g2}$  are the group velocities, normalized to  $c$ , of the structure wave at the interaction points  $C$  and  $A$ , respectively. The estimated value of Eq. (6) is about 3%. On the other hand, the value of  $\Delta V/V$  in the wave form shown in the inset of Fig. 2 is about 30%. The combined resonance may be turned off in a time scale of the voltage fluctuation. This is consistent with the observed output pulse duration from 50 to 150 nsec. The beam voltage fluctuation may also broaden the resonant magnetic field given by Eq. (3). When  $\Delta V/V$  is about 30%,  $\Delta B/B$  is expected to be about 27%, which is consistent with the observed broad resonance shown in Fig. 2 [15].

For the resonant magnetic field of Eq. (4), Cherenkov oscillation will synchronize with the normal Doppler cyclotron interaction. In the backward wave oscillator experiments, the Cherenkov radiations have been absorbed at this resonance [4,5]. In these cases, the axially streaming electrons gain a perpendicular energy. The possibility of the electronic efficiency enhancement has also been predicted theoretically [16,17]. For the efficiency enhancement, the axial electric fields of spacial harmonics in the SWS cavity should be adjusted very carefully or the TE mode, which can synchronize with the TM mode,

should exist. Neither condition was satisfied in our experiment.

With our experimental parameters, the estimated value of magnetic fields from Eq. (4) is around 0.43 T, in which no meaningful rf output was observed, as shown in Fig. 2. There was no Cherenkov radiation in this magnetic-field region, the cyclotron absorption could not be observed. The radiation due to the fast cyclotron interaction might not be expected for the following two reasons. Firstly, the ratio of the transverse velocity to the axial velocity of the beam electron estimated from the diode geometry is very small, less than 0.2. Secondly, the coupling of the fast cyclotron wave to the TM mode is reduced by the factor of  $v_z^2/c^2$  compared with the coupling to the TE mode [3,18]. This factor is very small in the weakly relativistic cases and is about 0.12 for the beam energy of 35 keV.

In the case of Eq. (5), three wave interactions involving Cherenkov, normal, and anomalous Doppler cyclotron modes will arise. With our experimental conditions, the resonant magnetic field is expected to be in the region of 1.2 T, in which we could not perform the experiments due to the limitation of our equipment. This combined resonance has not been analyzed previously in the literature to our knowledge. Theoretical and experimental studies are necessary in order to understand the basic features of the resonance.

In Ref. [19], a periodic metallic SWS consisting of an array of posts in a rectangular waveguide was successful-

ly used in a periodic ECM experiment in the relatively low-power regime. But this type of ECM is based on the normal Doppler cyclotron interaction,  $S=1$  in Eq. (2), independent of the Cherenkov mechanism and is essentially different from our slow-wave ECM. A kicker coil was required for the self-oscillation in contrast to our experiments, in which no special means for imparting transverse velocity to the beam electrons are used.

In conclusion, the high-power slow-wave ECM utilizing an oversized metallic SWS driven by an axially streaming electron beam has been operated successfully at the combined resonance of the Cherenkov and the anomalous Doppler cyclotron interactions. This is the first demonstration of the synergistic coupling between these two interactions. The high-power operation at beam voltage below 50 kV is unique and of considerable interest for practical use. The slow-wave ECM presented here may prove to be a candidate for a new type of useful microwave and millimeter wave source. A more definite study of the synergistic interactions described above should be made in the future using a power supply with a much lower value of voltage ripple.

#### ACKNOWLEDGEMENTS

The authors gratefully acknowledge helpful discussions with Dr. G. S. Nusinovich at the University of Maryland.

- 
- [1] *Applications of High-Power Microwaves*, edited by A. V. Gaponov-Grekhov and V. L. Granatstien (Artech House, Norwood, MA, 1994).
  - [2] J. L. Hirshfield and V. L. Grantstein, *IEEE Trans. Microwave Theory Tech.* **25**, 522 (1977).
  - [3] V. L. Bratman *et al.*, *Int. J. Electron.* **51**, 541 (1981).
  - [4] Y. Carmel *et al.*, *Phys. Fluids B* **4**, 286 (1992).
  - [5] J. A. Swegle *et al.*, *IEEE Trans. Plasma Sci.* **21**, 714 (1993).
  - [6] S. P. Bugaev *et al.*, *IEEE Trans. Plasma Sci.* **18**, 518 (1990), and references therein.
  - [7] N. S. Ginzburg, *Sov. Radiophys. Quantum Electron* **22**, 323 (1979).
  - [8] W. B. Case *et al.*, *J. Appl. Phys.* **55**, 2651 (1984).
  - [9] T. H. Kuo and A. T. Lin, *Phys. Rev. A* **38**, 2833 (1988).
  - [10] H. Guo *et al.*, *Phys. Rev. Lett.* **49**, 730 (1982).
  - [11] S. Yu. Galuzo *et al.*, *Zh. Tekh. Fiz.* **52**, 1681 (1982) [*Sov. Phys. Tech. Phys.* **27**, 1030 (1982)].
  - [12] A. N. Didenko *et al.*, *Pis'ma Zh. Tekh. Fiz.* **9**, 1331 (1983) [*Sov. Tech. Phys. Lett.* **9**, 572 (1983)].
  - [13] T. H. Kho and A. T. Lin, *IEEE Trans. Plasma Sci.* **18**, 13 (1990).
  - [14] K. Minami *et al.*, *IEEE Trans. Plasma Sci.* **23**, 124 (1995).
  - [15] This condition was pointed out by Dr. G. S. Nusinovich. In experiments on the X-band backward wave oscillator at the University of Maryland, an enhanced Cherenkov-cyclotron emission was observed by two of us (K.O. and Y.C.). Since  $\Delta V/V$  was small,  $\Delta B/B$  was less than a few percent as expected.
  - [16] A. Vlasov *et al.*, *Phys. Fluids B* **5**, 1625 (1993).
  - [17] G. S. Nusinovich and A. N. Vlasov, *Phys. Fluids B* **5**, 605 (1993).
  - [18] G. S. Ginzburg and G. S. Nusinovich, *Sov. Radiophys. Quantum Electron* **22**, 522 (1979).
  - [19] E. Jerby and G. Bekefi, *Phys. Rev. E* **48**, 4637 (1993).